

# Finding a Largest-Area Triangle in a Terrain in Near-Linear Time

Sergio Cabello<sup>1\*</sup>, Arun Kumar Das<sup>2</sup>, Sandip Das<sup>2</sup>, and Joydeep Mukherjee<sup>3</sup>

<sup>1</sup> Faculty of Mathematics and Physics, University of Ljubljana, Slovenia, and  
Institute of Mathematics, Physics and Mechanics, Slovenia.

<sup>2</sup> Advanced Computing and Microelectronics Unit, Indian Statistical Institute, India.

<sup>3</sup> Dept. of Computer Science, Ramakrishna Mission Vivekananda Educational and  
Research Institute, India.

**Abstract.** A terrain is an  $x$ -monotone polygon whose lower boundary is a single line segment. We present an algorithm to find in a terrain a triangle of largest area in  $O(n \log n)$  time, where  $n$  is the number of vertices defining the terrain. The best previous algorithm for this problem has a running time of  $O(n^2)$ .

**Keywords:** Terrain · Inclusion Problem · Geometric Optimisation · Hereditary Segment Tree

## 1 Introduction

An *inclusion problem* asks to find a geometric object inside a given polygon that is optimal with respect to a certain parameter of interest. This parameter can be the area, the perimeter or any other measure of the inner object that plays a role in the application at hand. Several variants of the inclusion problem come up depending on the parameter to optimize, the constraints imposed in the sought object, as well as the assumptions we can make about the containing polygon. For example, computing a largest area or largest perimeter convex polygon inside a given polygon is quite well studied [4,11,13]. A significant amount of work has also been done on computing largest-area triangle inside a given polygon [3,5,9,16]. The problems of finding largest area triangle [14,15] and largest area quadrilateral [17] inside a convex polygon are also studied recently. In this paper, we propose a deterministic  $O(n \log n)$ -time algorithm to find a largest-area triangle inside a given terrain, which improves the best known running time of  $O(n^2)$ , presented in [8]. These problems find applications in stock cutting [6], robot motion planning [18], occlusion culling [13] and many other domains of facility location and operational research.

A polygon  $P$  is  *$x$ -monotone* if it has no vertical edge and each vertical line intersects  $P$  in an interval, which may be empty. An  $x$ -monotone polygon has a unique vertex with locally minimum  $x$ -coordinate and a unique vertex with locally maximum  $x$ -coordinate; see for example [2, Lemma 3.4]. If we split the

---

\* Supported by the Slovenian Research Agency (P1-0297, J1-9109, J1-1693, J1-2452).

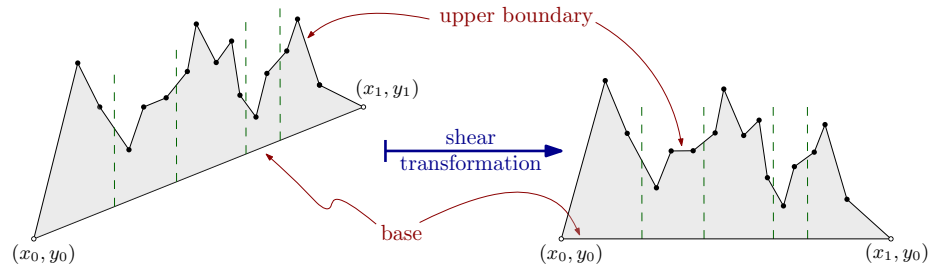


Fig. 1: Two terrains. The right one is obtained from the left one by a shear transformation to make the base horizontal

boundary of an  $x$ -monotone polygon at the unique vertices with maximum and minimum  $x$ -coordinate, we get the *upper boundary* and the *lower boundary* of the polygon. Each vertical line intersects each of those boundaries at most once.

A *terrain* is an  $x$ -monotone polygon whose lower boundary is a single line segment, called the *base* of the terrain. The upper boundary of the terrain is connecting the endpoints of the base and lies above the base: each vertical ray from the base upwards intersects the upper boundary at exactly one point. Figure 1 shows two examples.

In this work, we focus on the problem of finding inside a terrain a triangle of largest area. We will show that when the terrain has  $n$  vertices, such a largest-area triangle can be computed in  $O(n \log n)$  time. This is an improvement over the algorithm of Das et al. [8], which has a running time of  $O(n^2)$ . It should be noted that we compute a single triangle with largest area, even if there are more optimal solutions.

To obtain our new algorithm we build on the approach and geometric insights of [8]. More precisely, in that work, there is a single type of optimal solution that takes  $O(n^2)$  time, while all the other cases can be handled in  $O(n \log n)$  time. We show that the remaining case also can be solved in  $O(n \log n)$  time combining hereditary segment trees [7], search for row maxima in monotone matrices [1], and additional geometric insights.

Our new time bound,  $O(n \log n)$ , is a significant improvement over the best previous result. Nevertheless, the problem could be solvable in linear time, as we are not aware of any lower bound. We leave closing this gap as an interesting open problem for future research.

## 2 Preliminaries

Without loss of generality, we will assume that *the base of the terrain is horizontal*; the general case reduces to this one. Indeed, if the endpoints of the base are  $(x_0, y_0)$  and  $(x_1, y_1)$ , where it must be  $x_0 \neq x_1$ , then the shear mapping  $(x, y) \mapsto (x, y - (x - x_0) \frac{y_1 - y_0}{x_1 - x_0})$  transforms the base to the horizontal segment connecting  $(x_0, y_0)$  to  $(x_1, y_0)$ . Since the mapping also transforms each vertical

segment to a vertical segment, the terrain gets mapped to a terrain with a horizontal base; see Figure 1. Since the area of any measurable region of the plane is not changed with this affine transformation, because the determinant of the Jacobian matrix is 1, it suffices to find the triangle of largest area in the resulting polygon.

For simplicity, we will assume that *no three vertices in the terrain are collinear*. This property is invariant under shear transformations. The assumption can be lifted using simulation of simplicity [10].

A vertex of a terrain is *convex* if the internal angle between the edges incident to this vertex is less than  $180^\circ$ . If the angle is greater than  $180^\circ$ , then the vertex is *reflex*. Angles of  $180^\circ$  do not occur because of our assumption of no 3 collinear points. The endpoints of the base of the terrain are called *base vertices*. The one with smallest  $x$ -coordinate is the *left base vertex* and is denoted by  $B_\ell$ ; the one with largest  $x$ -coordinate is the *right base vertex* and is denoted by  $B_r$ . The base vertices are convex.

### 3 Previous geometric observations

In this section, we state several observations and properties given in [8], without repeating their proofs here. The first one talks about the structure of an optimal solution.

A triangle contained in the terrain with an edge on the base of the terrain is a *grounded triangle*. For a grounded triangle, the vertex not contained in the base of the terrain is the *apex*, and the edges incident to the apex are the *left side* and the *right side*; the right side is incident to the vertex of the base with larger  $x$ -coordinate.

**Lemma 1 (Lemmas 1 and 2, Corollary 1 in [8]).** *In each terrain there is a largest area triangle  $T$  satisfying all of the following properties:*

- (a) *the triangle  $T$  is grounded;*
- (b) *the apex of  $T$  lies on the boundary of the terrain or each of the left and right sides of  $T$  contains two vertices of the terrain.*

Note that property (b) splits into two cases. An option is that the apex of the grounded triangle is on the boundary of the terrain. The other option is that each of the edges incident to the apex contains two vertices of the terrain. The first case is already solved in  $O(n \log n)$  time.

**Lemma 2 (Implicit in [8]; see the paragraph before Theorem 1).** *Given a terrain with  $n$  vertices, we can find in  $O(n \log n)$  time the grounded triangle with largest area that has its apex on the boundary of the terrain.*

The key insight to obtain Lemma 3 is to decompose the upper boundary of the terrain into  $O(n)$  pieces with the following property: for any two points  $p, p'$  in the same piece, the largest grounded triangles with apex at  $p$  and with apex at  $p'$  have the same vertices of the terrain on the left and right sides.

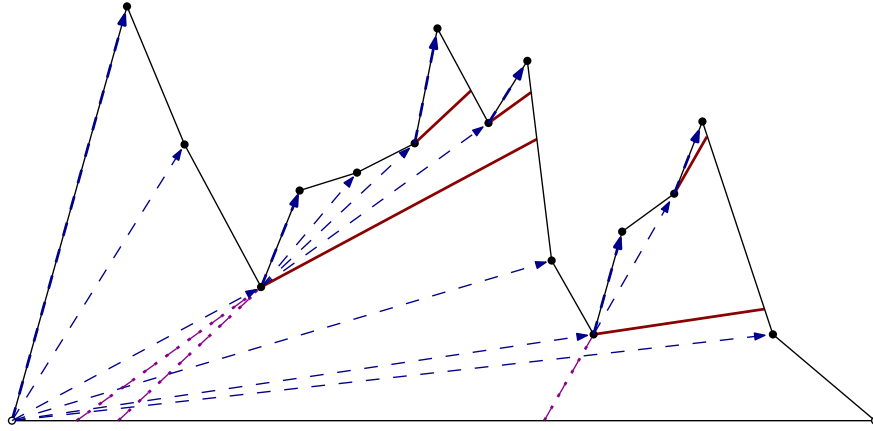


Fig. 2: The tree  $T_\ell$  with blue dashed arcs. The set  $L$ , of forward prolongations of the edges of  $E(T_\ell)$ , is in solid, thick red. In dashed-dotted purple is the set of backward prolongations for the edges defining  $L$ .

It remains the case when the apex is *not* contained on the boundary of the terrain. This means that each side of the optimal triangle contains two vertices of the terrain. There are two options: either both vertices contained in a side are reflex vertices, or one vertex is reflex and the other is a vertex of the base.

Recall that  $B_\ell$  is the left endpoint of the base of the terrain. Consider the visibility graph of the vertices of the terrain and let  $T_\ell$  be the shortest path tree from the vertex  $B_\ell$  in the visibility graph. We regard  $T_\ell$  as a geometric object, that is, a set of segments connecting vertices of the terrain. We orient the edges in  $T_\ell$  away from the root, consistent with the direction that the shortest path from  $B_\ell$  would follow them; see Figure 2.

Consider an (oriented) edge  $p \rightarrow q$  of  $T_\ell$ ; the point  $p$  is closer to  $B_\ell$  than  $q$  is; it may be that  $p = B_\ell$ . Its *forward prolongation* is the segment obtained by extending the directed segment  $p \rightarrow q$  until it reaches the boundary of the terrain. (The interior of the segment  $pq$  is not part of the prolongation.) Each point on the forward prolongation is further from  $B_\ell$  than  $q$  is. The *backward prolongation* of  $p \rightarrow q$  is the extension of  $p \rightarrow q$  from  $p$  in the direction  $q \rightarrow p$  until it reaches the boundary of the terrain. The forward prolongation is empty if  $q$  is a convex vertex, and the backwards extension is empty if  $p = B_\ell$ .

Let  $L$  be the set of non-zero-length forward prolongations of segments in  $T_\ell$ . See Figure 2. A similar construction is done to obtain a shortest-path tree  $T_r$  from the right endpoint  $B_r$  of the base of the terrain, the prolongations of its edges, and the set  $R$  of forward prolongations for the edges of  $T_r$ .

Using that the terrain is an  $x$ -monotone polygon and the lower boundary is a single segment, one obtains the following properties.

**Lemma 3 (Lemmas 3, 4 and 5 in [8]).** *The backward prolongation of each edge of  $E(T_\ell) \cup E(T_r)$  has an endpoint on the base of the terrain; it may be an*

endpoint of the base. The segments in  $E(T_\ell)$  have positive slope and the segments in  $E(T_r)$  have negative slope.

If the apex of the grounded triangle with largest area is not on the boundary of the terrain, then there is an edge  $s_\ell$  of  $L$  and an edge  $s_r$  of  $R$  such that: the left side of the triangle is collinear with  $s_\ell$ , the right side of the triangle is collinear with  $s_r$ , and the apex of the triangle is the intersection  $s_\ell \cap s_r$ .

## 4 New algorithm

We are now going to describe the new algorithm. In fact, we describe the missing piece in the previous approach of [8]. Because of Lemma 1, it suffices to search the grounded triangle of largest area. We have two cases to consider: the apex may be on the boundary of the terrain or not. The first case can be handled using Lemma 2. To approach the second case, we use Lemma 3: in such a case the apex of the triangle belongs to  $A = \{\ell \cap r \mid \ell \in L, r \in R\}$ .

We start providing a simple property for  $L$  and  $R$ .

**Lemma 4.** *The edges of  $L$  are pairwise interior-disjoint and can be computed in  $O(n)$  time. The same holds for  $R$ .*

*Proof.* Consider the forward prolongation  $qt \in L$  of the oriented edge  $p \rightarrow q$  of  $T_\ell$ . The shortest path from  $B_\ell$  to any point on  $qt$  consists of the shortest path from  $B_\ell$  to  $q$  followed by a portion of  $qt$ . It follows that the edges of  $L$  are contained in shortest paths from  $B_\ell$  and thus they are pairwise disjoint. (They cannot overlap because of our assumption on general position.)

Guibas et al. [12] show how to compute in  $O(n)$  time the shortest path tree  $T_\ell$  from  $B_\ell$  and the forward extensions  $L$ . This is the extended algorithm discussed after their Theorem 2.1, where they decompose the polygon into regions such that the shortest path to any point in the region goes through the same vertices of the polygon.  $\square$

We use Lemma 4 to compute  $L$  and  $R$  in linear time. Note that  $L \cup R$  has  $O(n)$  segments.

We use a *hereditary segment tree*, introduced by Chazelle et al. [7], as follows. We decompose the  $x$ -axis into intervals using the  $x$ -coordinates of the endpoints of the segments in  $L \cup R$ . We disregard the two unbounded intervals: the leftmost and the rightmost. The resulting intervals are called the *atomic intervals*. See Figure 3 for an example where the atomic intervals are marked as  $1, 2, \dots, 11$ . We make a height-balanced binary tree  $\mathcal{T}$  such that the  $i$ -th leaf represents the  $i$ -th atomic interval from left to right; see Figure 4. For each node  $v$  of the tree  $\mathcal{T}$ , we define the interval  $I_v$  as the union of all the intervals stored in the leaves of  $\mathcal{T}$  below  $v$ . Alternatively, for each internal node  $v$ , the interval  $I_v$  is the union of the intervals represented by its two children. In the two-dimensional setting,  $v$  represents the vertical strip bounded by the vertical lines passing through the end points of  $I_v$ . Let us denote this strip by  $J_v$ . In Figure 3,  $J_v$  is shaded in grey for the highlighted node in Figure 4.

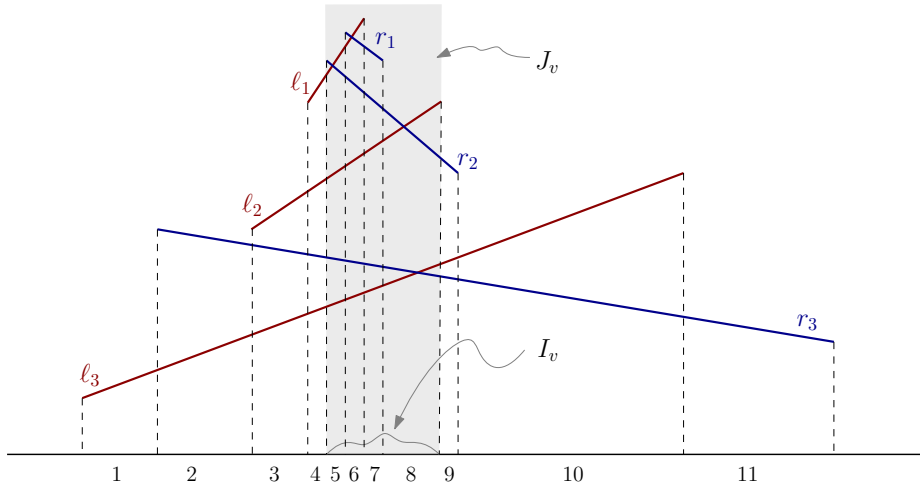


Fig. 3: Atomic intervals.

Consider a node  $v$  of  $\mathcal{T}$  and denote by  $w$  its parent. We maintain in  $v$  four lists of segments:  $L_v$ ,  $R_v$ ,  $L_v^h$  and  $R_v^h$ . The list  $L_v$  contains all the segments  $\ell \in L$  such that the  $x$ -projection of  $\ell$  contains  $I_v$  but does not contain  $I_w$ . Similarly,  $R_v$  contains the segments  $r \in R$  whose projection onto the  $x$ -axis contains  $I_v$  but does not contain  $I_w$ . We call  $L_v$  and  $R_v$  the *standard* lists. The list  $L_v^h$  contains the members of  $L_u$  for all proper descendants  $u$  of  $v$  in  $\mathcal{T}$ . Similarly,  $R_v^h$  contains the members of  $R_u$  for all proper descendants  $u$  of  $v$  in  $\mathcal{T}$ . We call  $L_v^h$  and  $R_v^h$  the *hereditary* lists. We put only one copy of a segment in a hereditary list of a node, even if it is stored in more than one of its descendants. See Figure 4 for an example. All the members of the standard lists of each node are stored inside the relevant node. The members of  $L$  are colored as red and the members of  $R$  are colored as blue.

Chazelle et al. [7] noted that

$$\sum_v (|L_v| + |R_v| + |L_v^h| + |R_v^h|) = O(n \log n). \quad (1)$$

Indeed, each single segment  $s$  of  $L \cup R$  appears in  $O(\log n)$  standard lists, namely in at most two nodes at each level. Moreover, the nodes that contain  $s$  in their standard lists have  $O(\log n)$  ancestors in total, namely the search nodes on the search path to the extreme atomic intervals contained in projection of  $s$ . It follows that  $s$  appears in  $O(\log n)$  hereditary lists.

For each node  $v$  of  $\mathcal{T}$  we define the intersections

$$\begin{aligned} A_v = & \{ \ell \cap r \mid \ell \in L_v, r \in R_v, x(\ell \cap r) \in I_v \} \cup \\ & \{ \ell \cap r \mid \ell \in L_v^h, r \in R_v, x(\ell \cap r) \in I_v \} \cup \\ & \{ \ell \cap r \mid \ell \in L_v, r \in R_v^h, x(\ell \cap r) \in I_v \}. \end{aligned}$$

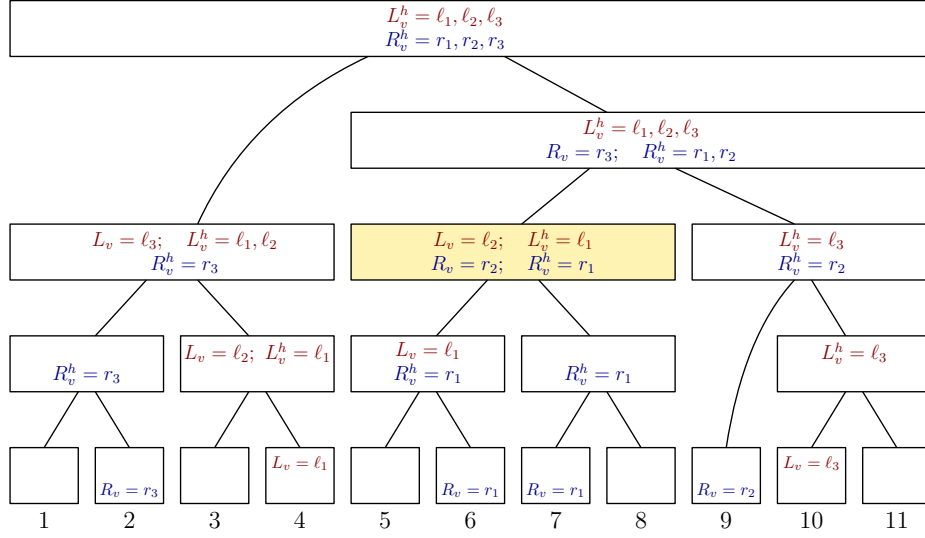


Fig. 4: Example of hereditary segment tree for Figure 3. All the lists that are not indicated are empty.

**Lemma 5.** *The set  $A$  is the (disjoint) union of the sets  $A_v$ , where  $v$  iterates over the nodes of  $\mathcal{T}$ .*

*Proof.* Consider a pair of intersecting segments  $\ell \in L$  and  $r \in R$ , and let  $u$  be the leaf of  $\mathcal{T}$  such that the  $x$ -coordinate of  $\ell \cap r$  is contained in  $I_u$ . We walk from  $u$  upwards along the tree until the first node  $v$  with the property that  $\ell \in L_v \cup L_v^h$  and  $r \in R_v \cup R_v^h$  is reached. It cannot be that  $\ell \in L_v^h$  and  $r \in R_v^h$  because otherwise both  $\ell$  and  $r$  would be in the lists of the descendant of  $v$  towards the leaf  $u$ . Moreover, the intersection point  $\ell \cap r$  has its  $x$ -coordinate in  $I_v$  because  $x(\ell \cap r) \in I_u \subseteq I_v$ . It follows that  $\ell \cap r \in A_v$ .  $\square$

We have to find the best apex in  $A$ . Since  $A = \bigcup_v A_v$  because of Lemma 5, it suffices to find the best apex in  $A_v$  for each  $v$ . For this we consider each  $v$  separately and look at the interaction between the lists  $L_v$  and  $R_v$ ,  $L_v^h$  and  $R_v$ ,  $R_v^h$  and  $L_v$ .

#### 4.1 Interaction between two standard lists

Consider a fixed node  $v$  and its standard lists  $L_v$  and  $R_v$ . The  $x$ -projection of each segment in  $L_v \cup R_v$  is a superset of the interval  $I_v$ , and thus no endpoint of such a segment lies in the interior  $J_v$ .

Since the segments in  $L_v$  are pairwise interior-disjoint (Lemma 4) we can sort them with respect to their  $y$ -order within  $I_v$ . We sort them in decreasing  $y$ -order. Henceforth, we regard  $L_v$  as a sorted list. Thus,  $L_v$  contains  $\ell_1, \dots, \ell_{|L_v|}$  and, whenever  $1 \leq i < j \leq |L_v|$ , the segment  $\ell_i$  is above  $\ell_j$ . We do the same for

$R_v$ , also by decreasing  $y$ -coordinate. Thus,  $R_v$  is a sorted list  $r_1, \dots, r_{|R_v|}$  and, whenever  $1 \leq i < j \leq |R_v|$ , the segment  $r_i$  is above  $r_j$ .

Because of Lemma 3, each segment  $s$  of  $L \cup R$  can be prolonged inside the terrain until it hits the base of the terrain. Indeed, such a prolongation contains an edge of  $E(T_\ell) \cup E(T_r)$  by definition. Let  $b(s)$  be the point where the prolongation of  $s$  intersects the base of the terrain.

**Lemma 6.** *If  $1 \leq i < j \leq |L_v|$ , then  $b(\ell_i)$  lies to the right of  $b(\ell_j)$ . If  $1 \leq i < j \leq |R_v|$ , then  $b(r_i)$  lies to the left of  $b(r_j)$ .*

*Proof.* Let  $s_i$  be the longest segment that contains  $\ell_i$  and is contained in the terrain; let  $s_j$  be the longest segment that contains  $\ell_j$  that is contained in the terrain. Thus  $b(\ell_i)$  is an endpoint of  $s_i$  and  $b(\ell_j)$  is an endpoint of  $s_j$ . Assume, for the sake of reaching a contradiction, that  $b(\ell_i)$  lies to the left of  $b(\ell_j)$ . This means  $s_i$  and  $s_j$  are disjoint, and thus  $s_i$  is completely above  $s_j$  for any  $x$ -coordinate that they share. Then  $s_j$  cannot go through any vertex of the terrain to the left of  $J_v$ , as such a vertex would be below  $s_i$ , which is contained in the terrain. By construction of the hereditary segment tree  $I_v$  is a proper subset of the  $x$ -projections of  $\ell_j$  and none of the end points of  $\ell_j$  belongs to interior of  $J_v$ . This means the left end point of the  $\ell_j$  should be to the left of  $J_v$ . Hence we arrive at the contradiction.

The argument for segments of  $R$  is similar. □

Once  $L_v$  and  $R_v$  are sorted, we can detect in  $O(|L_v| + |R_v|)$  time which segments of  $L_v$  do not cross any segment of  $R_v$  inside  $J_v$ . Indeed, we can merge the lists to obtain the order  $\pi_\ell$  of  $L_v \cup R_v$  along the left boundary of  $J_v$  and the order  $\pi_r$  along the right boundary of  $J_v$ . Then we note that  $\ell_i$  does not intersect any segment of  $R_v$  inside  $J_v$  if and only if the ranking of  $\ell_i$  is the same in  $\pi_\ell$  and in  $\pi_r$ . We remove from  $L_v$  the segments that do not cross any segment of  $R_v$  inside  $J_v$ . To avoid introducing additional notation, we keep denoting to the resulting list as  $L_v$ .

Within the same running time  $O(|L_v| + |R_v|)$  time we can find for each  $\ell_i \in L_v$  an index  $\psi(i)$  such that  $\ell_i$  and  $r_{\psi(i)}$  intersect inside  $J_v$ . Indeed, if  $\ell_i$  crosses some segment of  $R_v$  inside  $J_v$ , then it must cross one of the segments of  $R_v$  that is closest to  $\ell_i$  in the order  $\pi_\ell$  (the predecessor or the successor from  $R_v$ ). These two candidates for all  $\ell_i$  can be computed with a scan of the order  $\pi_\ell$ .

Consider the  $|L_v| \times |R_v|$  matrix  $M = (M[i, j])_{i, j}$  defined as follows. If  $\ell_i$  and  $r_j$  intersect in  $J_v$ , then  $M[i, j]$  is the area of the grounded triangle with apex  $\ell_i \cap r_j$  and sides containing  $\ell_i$  and  $r_j$ . If  $\ell_i$  and  $r_j$  do not intersect in  $J_v$ , and  $j < \psi(i)$ , then  $M[i, j] = j\varepsilon$  for an infinitesimal  $\varepsilon > 0$ . In the remaining case, when  $\ell_i$  and  $r_j$  do not intersect in  $J_v$  but  $\psi(i) < j$ , then  $M[i, j] = -j\varepsilon$  for the same infinitesimal  $\varepsilon > 0$ . Thus, a generic row of  $M$ , when we walk it from left to right, has small positive increasing values until it reaches values defined by the area of triangles, and then it starts taking small negative values that decrease. The matrix  $M$  is not constructed explicitly, but we work with it implicitly. Given a pair of indices  $(i, j)$ , we can compute  $M[i, j]$  in constant time.



Note that within each row of  $M$  the non-infinitesimal elements are contiguous. Indeed, Whether a segment of  $L_v$  and a segment of  $R_v$  intersect in  $J_v$  depends only on the orders  $\pi_\ell$  and  $\pi_r$  along the boundaries of  $J_v$ , which is the same as the order along the lists  $L_v$  and  $R_v$ . It also follows that the entries of  $M$  defined as areas of triangles form a staircase such that in lower rows it moves towards the right.

The following property shows that  $M$  is totally monotone.

**Lemma 7.** *Consider indices  $i, i', j, j'$  such that  $1 \leq i < i' \leq |L_v|$  and  $1 \leq j < j' \leq |R_v|$ . If  $M[i', j] > M[i', j']$ , then  $M[i, j] > M[i, j']$ .*

*Proof.* The cases when  $s_{i'}$  and  $\ell_j$  do not intersect or  $s_i$  and  $\ell_{j'}$  do not intersect are treated by a case analysis. For example,  $s_{i'}$  and  $\ell_j$  do not intersect, then  $M[i', j] > M[i', j']$  can only occur when  $\psi(i') < j < j'$ . In such a case  $\ell_i$  cannot intersect  $r_j$  neither  $r_{j'}$  and we must have also  $\psi(i) < j < j'$ . Thus  $M[i, j] = -j\varepsilon > -j'\varepsilon = M[i, j']$ .

The argument when  $s_i$  and  $\ell_{j'}$  do not intersect is similar, but using the contrapositive. If  $M[i, j] \leq M[i, j']$ , then both  $j, j'$  must be to the left of  $\psi(i)$  and  $s_i$  does not intersect  $r_j$  nor  $r_{j'}$ . In such a case  $\ell_{i'}$  cannot cross  $s_j$  nor  $s_{j'}$ .

It remains the interesting case, when  $\ell_{i'}$  and  $r_j$  intersect and also  $\ell_i$  and  $r_{j'}$  intersect. Using that  $\ell_i$  is above  $\ell_{i'}$ , that  $r_j$  is above  $r_{j'}$ , that  $\ell_{i'}$  intersects  $r_j$ , and that  $\ell_i$  intersects  $r_{j'}$ , we conclude that  $\ell_i$  also intersects  $r_j$  and that  $\ell_{i'}$  also intersects  $r_{j'}$ . For this we just have to observe the relative order of the endpoints of the segments restricted to the boundaries of  $J_v$ .

Next we use elementary geometry, as follows. See Figure 5. Because of Lemma 6, the extensions of  $\ell_i$  and  $\ell_{i'}$  inside the terrain intersect in a point to the left of  $J_v$ , which we denote by  $p_\ell$ . Similarly, the extensions of  $r_j$  and  $r_{j'}$  intersect in a point  $p_r$  to the right of  $J_v$ .

For each  $(\alpha, \beta) \in \{i, i'\} \times \{j, j'\}$ , let  $a_{\alpha, \beta}$  be the intersection point of  $\ell_\alpha$  and  $r_{\varphi(\beta)}$ . Thus, we have defined four points, namely  $a_{i, j}, a_{i, j'}, a_{i', j}, a_{i', j'}$ . We have argued before that these four points indeed exist, and they lie in  $J_v$ . We also define the triangle  $T_{\alpha, \beta}$  as the grounded triangle with sides containing  $\ell_\alpha$  and  $r_{\varphi(\beta)}$  (and thus apex  $a_{\alpha, \beta}$ ).

We define the following areas

$$\begin{aligned} A_1 &= \text{area}(\triangle(b(\ell_{i'}), b(\ell_i), p_\ell)), & A_2 &= \text{area}(\triangle(p_\ell, a_{i', j'}, a_{i, j'})) \\ A_3 &= \text{area}(\diamond(a_{i, j'}, a_{i', j'}, a_{i', j}, a_{i, j})), & A_4 &= \text{area}(\triangle(p_r, a_{i', j'}, p_\ell)) \\ A_5 &= \text{area}(\triangle(a_{i', j'}, p_r, a_{i', j})), & A_6 &= \text{area}(\triangle(b(r_j), b(r_{j'}), p_r)). \end{aligned}$$

The condition  $M[i', j] > M[i', j']$  translates into

$$A_1 + A_4 + A_5 = M[i', j] > M[i', j'] = A_1 + A_4 + A_6,$$

which implies that  $A_5 > A_6$ . We then have

$$M[i, j] = A_2 + A_3 + A_4 + A_5 > A_2 + A_3 + A_4 + A_6 > M[i, j']$$

as we wanted to show.  $\square$

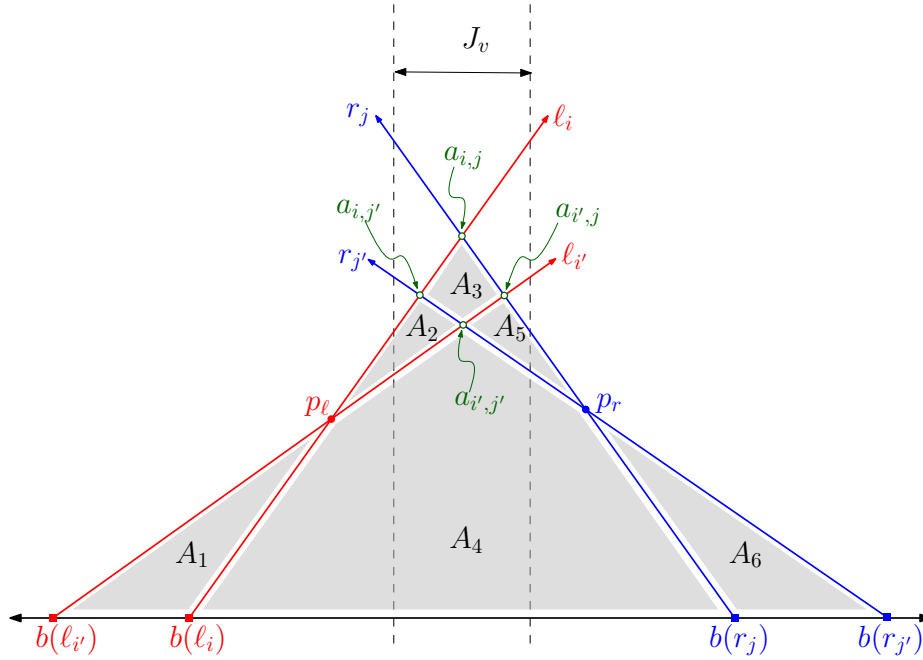


Fig. 5: Scenario in the proof of Lemma 7.

For each index  $i$  with  $1 \leq i \leq |L_v|$ , let  $\varphi(i)$  be the smallest index of columns where the maximum in the  $i$ th arrow of  $M$  is attained. Thus,  $M_{i,\varphi(i)} = \max\{M_{i,j} \mid 1 \leq j \leq |R_v|\}$ . Since  $M$  is totally monotone, we can compute the values  $\varphi(i)$  for all  $1 \leq i \leq |L_v|$  using the SWAMK algorithm of Aggarwal et al. [1]. This step takes  $O(|L_v| + |R_v|)$  time.

We return the maximum among the values  $M[i, \varphi(i)]$ . In total we have spent  $O(|L_v| + |R_v|)$  time, assuming that  $L_v$  and  $R_v$  were in sorted form.

#### 4.2 Interaction between a standard list and a hereditary list

Consider now a fixed node  $v$ , its standard list  $L_v$  and its hereditary list  $R_v^h$ . The  $x$ -projection of each segment in  $L_v$  is a superset of the interval  $I_v$ , and thus no endpoint of such a segment lies in the interior of  $J_v$ . However, the  $x$ -projection of a segment in  $R_v^h$  has non empty intersection with the interval  $I_v$ , but it is not a superset of  $I_v$ . This implies that each segment of  $R_v^h$  has at least one of its endpoints in the interior of  $J_v$ .

**Observation 1.** *No endpoint of any segment  $r_j \in R_v^h$  can be present inside the strip  $J_v$  and below any segment of  $L_v$ .*

*Proof.* The vertical upwards ray from the endpoint is outside the terrain, because the endpoint is on the boundary of the terrain, while the segments of  $L_v$  are contained in the terrain.  $\square$

We only consider those segments of  $R_v^h$  which have their right endpoint on the exterior or on the right boundary of  $J_v$  and this right endpoint lies below the right endpoint of the topmost member of  $L_v$  in  $J_v$ . These are the members who participate in forming a feasible grounded triangle by interacting with the members of  $L_v$ .

**Observation 2.** *Let  $p$  be the point where the top most member of  $L_v$  intersects the right boundary of  $J_v$ . If  $r'_i \in R_v^h$  intersects the right boundary of  $J_v$  below  $p$  then  $r'_i$  must have its left end point above the top most member of  $L_v$ .*

*Proof.* If any of such left end point  $q$  is present below any segment of  $L_v$  then the perpendicular through that point on the terrain base intersects the members of  $L_v$ , who are lying above  $q$ , outside the terrain. This is a contradiction as lies on the boundary of the terrain.  $\square$

Like before, we assume that the members of  $L_v$  are sorted by decreasing  $y$ -order. We also assume that the relevant elements of  $R_v^h$  are sorted by  $y$ -coordinate along their intersection with the right boundary of  $J_v$ .

Using Observations 1 and 2 and an argument similar to Lemma 7 we can establish that these sorted members satisfy a totally monotone property. Indeed, the segments of  $R_v^h$  do not cross the whole  $J_v$  but they cannot finish with an endpoint in  $J_v$  below an element of  $L_v$ . This suffices to argue that the crossings used in the proof of Lemma 7 exist. Thus finding a largest area grounded triangle formed by the members of the sorted lists  $L_v$  and  $R_v^h$  needs  $O(|L_v| + |R_v^h|)$  amount of time. We can also handle the interaction between  $R_v$  and  $L_v^h$  in a similar fashion. This finishes the description of the interaction between a standard and a hereditary list in a node  $v$ .

### 4.3 Putting things together

Because of Lemma 5, by handling the interactions between the standard lists at each node  $v$  of  $\mathcal{T}$  and between the standard list and each of the hereditary lists, we find an optimal triangle whose apex lies in  $A$ .

To get the lists sorted at each node, we can use the same technique that Chazelle et. al [7] used to improve their running time. We define a partial order in the segments of  $L$ : a segment  $\ell$  is a predecessor of  $\ell'$  if they share some  $x$ -coordinate and  $\ell$  is above  $\ell'$  at the common  $x$ -coordinate, or if they do not share any  $x$ -coordinate and  $\ell$  is to the left of  $\ell'$ . One can see that this definition is transitive and can be extended to a total order. This partial order can be computed with a sweep line algorithm and extended to a total order using a topological sort. Once this total order is computed at the root, it can be passed to its descendants in time proportional to the lists. (We compute this for  $L$  and for  $R$  separately.)

**Theorem 1.** *A largest area triangle inside a terrain with  $n$  vertices can be found in  $O(n \log n)$  time.*

*Proof.* The computation of the total order extending the above-below relation takes  $O(n \log n)$  for  $L$  and for  $R$ . After this, we can pass the sorted lists to each child in time proportional to the size of the lists. Thus, we spend additional  $O(|L_v| + |R_v| + |L_v^h| + |R_v^h|)$  time per node  $v$  of the hereditary tree to get the sorted lists.

Once the lists at each node  $v$  of the hereditary tree are sorted, we spend  $O(|L_v| + |R_v| + |L_v^h| + |R_v^h|)$  time to handle the apices of  $A_v$ , as explained above. Using (1), the total time over all nodes together is  $O(n \log n)$ .  $\square$

## References

1. Aggarwal, A., Klawe, M., Moran, S., Shor, P., Wilber, R.: Geometric applications of a matrix-searching algorithm. *Algorithmica* **2**, 195–208 (01 1987)
2. de Berg, M., Cheong, O., van Kreveld, M.J., Overmars, M.H.: *Computational Geometry: Algorithms and Applications*. Springer, 3rd edn. (2008)
3. Boyce, J.E., Dobkin, D.P., Drysdale, III, R.L., Guibas, L.J.: Finding extremal polygons. In: STOC. pp. 282–289. ACM (1982)
4. Cabello, S., Cheong, O., Knauer, C., Schlipf, L.: Finding largest rectangles in convex polygons. *Comput. Geom. Theory Appl.* **51**(C), 67–74 (2016)
5. Chandran, S., Mount, D.: A parallel algorithm for enclosed and enclosing triangles. *Int. J. Comput. Geometry Appl.* **2**, 191–214 (1992)
6. Chang, J.S., Yap, C.K.: A polynomial solution for the potato-peeling problem. *Discrete & Computational Geometry* **1**(2), 155–182 (1986)
7. Chazelle, B., Edelsbrunner, H., Guibas, L., Sharir, M.: Algorithms for bichromatic line-segment problems polyhedral terrains. *Algorithmica* **11**, 116–132 (02 1994)
8. Das, A.K., Das, S., Mukherjee, J.: Largest triangle inside a terrain. *Theoretical Computer Science* **858**, 90–99 (2021)
9. Dobkin, D.P., Snyder, L.: On a general method for maximizing and minimizing among certain geometric problems. In: SFCS. pp. 9–17 (1979)
10. Edelsbrunner, H., Mücke, E.P.: Simulation of simplicity: a technique to cope with degenerate cases in geometric algorithms. *ACM Trans. Graph.* **9**(1), 66–104 (1990)
11. Goodman, J.E.: On the largest convex polygon contained in a non-convex  $n$ -gon, or how to peel a potato. *Geometriae Dedicata* **11**(1), 99–106 (1981)
12. Guibas, L.J., Hershberger, J., Leven, D., Sharir, M., Tarjan, R.E.: Linear-time algorithms for visibility and shortest path problems inside triangulated simple polygons. *Algorithmica* **2**, 209–233 (1987)
13. Hall-Holt, O., Katz, M.J., Kumar, P., Mitchell, J.S.B., Sityon, A.: Finding large sticks and potatoes in polygons. In: SODA. pp. 474–483 (2006)
14. van der Hoog, I., Keikha, V., Löffler, M., Mohades, A., Urhausen, J.: Maximum-area triangle in a convex polygon, revisited. *Information Processing Letters* **161**, 105943 (2020)
15. Kallus, Y.: A linear-time algorithm for the maximum-area inscribed triangle in a convex polygon (2017)
16. Melissaratos, E., Souvaine, D.: Shortest paths help solve geometric optimization problems in planar regions. *SIAM Journal on Computing* **21**(4), 601–638 (1992)
17. Rote, G.: The largest contained quadrilateral and the smallest enclosing parallelogram of a convex polygon (2019)
18. Toth, C.D., O’Rourke, J., Goodman, J.E.: *Handbook of discrete and computational geometry*. CRC press (2017)